Hydrological Processes

WILEY

RESEARCH ARTICLE OPEN ACCESS

Simulation of Complex Groundwater Flow Processes in Low-Fidelity Radial Flow Model Using a Mathematical Representation of the Variation of Vertical Hydraulic Conductivity With Depth

Majdi Mansour[1] | Vasileios Christelis[1] | Kirsty Upton[2] | Andrew Hughes[1]

[1]British Geological Survey, Environmental Science Centre, Keyworth, UK | [2]British Geological Survey, Lyell Centre, Edinburgh, UK

Correspondence: Majdi Mansour (majm@bgs.ac.uk)

Received: 4 March 2024 | **Revised:** 10 December 2024 | **Accepted:** 11 December 2024

Funding: This work was supported by the UK Research and Innovation.

Keywords: deployable output | fractured aquifer | groundwater | radial flow model | variation of hydraulic conductivity with depth

ABSTRACT

Numerical groundwater models are key tools to calculate the deployable output from pumped boreholes. Their calibration requires undertaking multiple runs to optimise the parameter values. To maintain computational efficiency, the hydrogeological complexity of fractured and weathered aquifers is often represented in numerical models using a simplified approach consisting of a mathematical equation that describes the vertical variation of horizontal hydraulic conductivity (K_h) value with depth. In this article, we present the inclusion of the variation of the vertical hydraulic conductivity (K_v) with depth to a radial flow model. We derive the mathematical equation controlling the flow vertically between the numerical nodes. We show that the inclusion of K_v variation with depth have a limited impact on the shape of the time drawdown curve at the early times of a pumping test but its significance is higher at later times. This also has a measurable impact on the water level inside the pumped borehole especially when the variations of both K_h and K_v are accounted for. We use a simple linear variation of K_v with depth but the method is also applicable to complex profile of aquifer heterogeneity if this complexity can be represented using polynomial approximation. This illustrates the applicability of the proposed method to a wide range of weathered aquifer settings.

1 | Introduction

A considerable number of aquifers across the world characterised as fractured, weathered or karstic provide a major source of fresh water for public or industrial use (Owor et al. 2022, Upton et al. 2020). Under extreme dry conditions, groundwater may become the only means of water supply to buffer the adverse environmental and societal impacts of drought events (Calow et al. 2010). Groundwater is typically exploited by borehole pumping and for resource management, their yield must be calculated under different climatic conditions.

In the UK, reliable yields from boreholes are estimated using methods that use curves derived from measured operational data for borehole water levels and pumping rates (Grout, Alexander, and Simpson 1992; Beeson, Misstear, and van Wonderen 1997; Misstear and Beeson 2000). To account for climate change, these methods involve shifting the curve to new positions using a subjective assessment based on expert judgement. An example of borehole yield calculation is provided by Ascott et al. (2019) for both historical and projected conditions. Ascott et al. (2019) showed that in complex fractured or weathered aquifers, this expert-based approach

can be challenged as it may not account for all flow processes. Their study examined the yield of boreholes drilled in the limestone aquifers including Cretaceous-age Chalk of the UK, which are fractured with a decreasing permeability with depth (Rushton, 1976, Rushton and Rathod 1981, Grout, Alexander, and Simpson 1992, Taylor, 2001, Jackson 2002, Soley et al. 2012, Tamayo-Mas, Bianchi, and Mansour 2018). To improve yield calculation, they used a radial numerical model (Mansour et al. 2011) that simulates the fluctuations of water levels inside the pumped borehole.

Assessment of borehole yields in weathered aquifers in Ghana, Africa, is presented by Bianchi et al. (2020) and undertaken using a multilayered MODFLOW model (Harbaugh, 2005). Numerical models are computationally costly when they are used to simulate large numbers of complex 3D aquifer settings to optimise the solution or undertake uncertainty analysis. The advancement of computing power and the development of new techniques that improve the representation of hydraulic features in numerical solutions, for example, the implementation of unstructured grid in MODFLOW6 (Langevin et al. 2022), reduce the model size but still requires large numbers of layers to include vertical heterogeneity. Low-fidelity (LF) models, those that simplify the physics or reduce the dimensionality, for example, are used effectively in water resources management studies to address the computational burden arising from complex models (Asher et al. 2015; Christelis and Hughes 2022; Christelis et al. 2023). The model used by Ascott et al. (2019) can be categorised as a LF model as it is built in a two-numerical layer configuration only and accounts for vertical heterogeneity using an analytical equation that calculates the transmissivity value based on the simulated groundwater head. This approach is termed the vertical hydraulic conductivity with depth (VKD) approach hereafter (Rushton and Rathod 1981; Rushton, Connorton, and Tomlinson 1989). In this configuration, the model is simple, numerically stable and includes the main hydrogeological features that characterise fractured or weathered aquifers and provide reasonable solutions on reduced computational cost.

When the VKD approach is applied (see, for example, Rushton and Rathod 1981, Grout, Alexander, and Simpson 1992, Taylor, 2001, Jackson 2002, Soley et al. 2012), the horizontal hydraulic conductivity is the only hydraulic parameter that is made to vary with depth. This may be deemed acceptable when groundwater flows are simulated for groundwater resources assessment at regional scales. However, for the assessment of borehole yield under drought conditions, when groundwater levels drop significantly, the variations of the storage coefficient and the vertical hydraulic conductivity values with depth will have an impact on the water table response in the vicinity of the borehole.

Rushton and Chan (1976) show the benefits of varying both the horizontal hydraulic conductivity and the storage coefficient with depth to simulate two pumping tests of a borehole starting from two different rest water levels. They conclude that the variations of both these hydraulic processes with depth must be accounted for to improve the model performance. In unconfined aquifers, the delayed yield concept, which consists of adding an exponential term in the analytical solution (Boulton 1954) is used to reproduce the shapes of the time drawdown curves. However, this time-drawdown behaviour is reproduced in numerical models by adding the water table as a boundary condition as shown by Mansour et al. (2011). In this case, the water table nodes are not connected to the pumped borehole directly, rather they are connected to the other aquifer nodes using the vertical hydraulic parameter. This demonstrates that the vertical hydraulic conductivity has a significant impact on the groundwater levels inside the pumped borehole and its vertical variation in fractured or weathered aquifers must be also included in LF models.

The aim of this study is to update the radial flow models used in LF configuration to improve the calculation of borehole yields by accounting for the variation of K_v with depth. First, we show the impact of the vertical hydraulic connectivity between the nodes on the shape of the time drawdown curves obtained from pumping tests and on the groundwater flow processes in terms of which part of the aquifer is contributing water to the pumped borehole. A mathematical equation that allows the calculation of vertical flow between numerical cells is then derived based on a linear variation of K_v with depth. Finally, hypothetical models are developed to demonstrate the implications of adding the vertical variation of K_v on the calculated groundwater levels and borehole yields and consequently groundwater resources assessment.

2 | Methodology and Justifications

2.1 | Description of the Numerical Model

The numerical model used to simulate the groundwater flows in the aquifer is a finite difference model built using a cylindrical grid (Mansour, Hughes, and Spink 2007). The model solves the implicit numerical form of the three-dimensional governing flow equation in porous media given by

$$\frac{K_r}{r}\frac{\partial h}{\partial r}+\frac{\partial}{\partial r}\left(\frac{K_r}{r}\frac{\partial h}{\partial r}\right)+\frac{1}{r}\frac{\partial}{\partial \theta}\left(K_\theta\frac{\partial h}{\partial \theta}\right)+\frac{\partial}{\partial z}\left(K_z\frac{\partial h}{\partial z}\right)+N=S_s\frac{\partial h}{\partial t}, \tag{1}$$

where $h(r,\theta,z)$ is the hydraulic head [L] at a point at cylindrical coordinates (r,θ,z), S_s is the specific storage [L^{-1}], N is a sink-source per unit volume term that is positive for recharge and negative for withdrawal [T^{-1}] and K_r, K_θ and K_z represent the hydraulic conductivity values [LT^{-1}] along the respective cylindrical coordinate directions: r the radial direction from the centre of the aquifer and outwards, θ the circumferential direction and z the vertical direction.

In this model, the pumped borehole is located at the centre of the numerical grid. The nodes are distributed along the radial directions with the spacing between them increasing in a logarithmic pattern from the borehole and towards the outer boundary. This numerical distribution of grid nodes increases node number in the vicinity of the pumped borehole leading to a more accurate representation of the steep hydraulic gradients adjacent to the borehole.

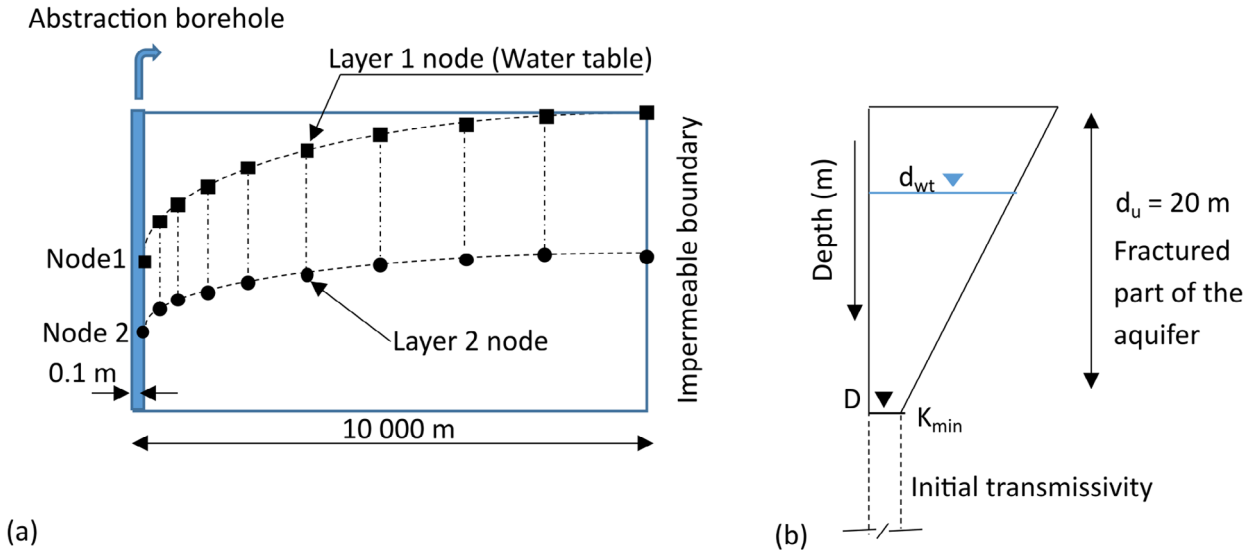

FIGURE 1 | (a) A simple numerical model configuration. (b) Example of variation of the hydraulic conductivity with depth.

In an unconfined aquifer, a numerical layer is added at the top of the upper numerical layer of the saturated zone to simulate the moving water table surface. Figure 1a shows a simple two-dimensional representation of the model with a numerical layer at the middle of the saturated layer and a second layer above it representing the water table. The specific storage S_s is used to control the storage terms of the numerical equation applied to nodes in Layer 2 in Figure 1a. For nodes in Layer 1 (the water table), the storage coefficient is set to the value of the specific yield S_y.

Vertical variation of the horizontal hydraulic conductivity with depth (VKD) is incorporated in the model using the method developed by Rushton, Connorton, and Tomlinson (1989). In this case, the transmissivity of the total saturated profile is calculated using Equation 2 assuming that the VKD profile is represented by the solid lines in Figure 1b (Ascott et al. 2019).

$$T = K_{min} c \left(\frac{(\mathrm{D} - d_{wt})^2}{2} \right), \tag{2}$$

where K_{min} and K_{max} are the horizontal hydraulic conductivity values at the base and top of the VKD profile, respectively, c is defined as $\left(\frac{(K_{max} - K_{min}) / K_{min}}{d_u} \right)$, d_u is the depth of the fractured part of the aquifer and over which K_v is assumed to vary linearly. d_{wt} is the depth of the water table and D is the depth of the base of the aquifer.

The abstraction rate is allocated at a node inside the pumped borehole, which is linked to the numerical layer in the middle of the aquifer only (Node 2 in Figure 1a) using a high hydraulic conductivity value. The drawdown values inside the pumped borehole and Node 2 are, therefore, the same. The extra node inside the well is allocated a storage coefficient value that represents well storage. This node is not connected to the layer representing the water table (Node 1 in Figure 1a). Assuming radial symmetry, that is no changes in the aquifer hydrological characteristics circumferentially, then the circumferential (θ) term in Equation 1 can be dropped and the flow is simulated in the radial and vertical dimensions only. This represents the simplest form that this model can take when unconfined aquifer flows are simulated, and this is the LF numerical model that will be used in all the simulations hereafter.

The grid nodes are vertically connected with a conductance term that is calculated using the vertical hydraulic conductivity value. Pumping causes the deformation of the numerical grid as shown in Figure 1a, which leads to changes in the saturated thickness and the conductance values controlling the flows between the nodes. The conductance values are updated at every time step when a new position of the water table is obtained.

The model output has been benchmarked against analytical steady-state solutions and transient solutions such as Theis (1935) and Neuman (1972) for confined and unconfined aquifers, respectively (Mansour, Hughes, and Spink 2007).

2.2 | Justification for Varying the Vertical Hydraulic Conductivity (K_v) With Depth

The need for varying the vertical hydraulic conductivity value with depth in fractured aquifers is demonstrated based on its impact on the shape of the time drawdown curves and the analysis of the water balance simulated by the numerical model at the discrete volumes of the model grid.

At the onset of pumping, the water level inside the pumped borehole starts to drop. The speed of this water level drop depends on the pumping rate, the size of the borehole and its storage capacity and the rate of groundwater release from the aquifer into the borehole. The latter depends on the hydraulic gradients established within the aquifer and its hydraulic characteristics. Consequently, the shape of the time drawdown curve observed at the pumped borehole becomes a function of the pumped borehole physical characteristics and

TABLE 1 | Aquifer depth and hydraulic parameter values used to produce the plots in Figure 2.

Parameter	Value
Aquifer depth (m)	20
Horizontal hydraulic conductivity (m/d)	50
Vertical hydraulic conductivity (m/d)	0.05
Specific storage (m^{-1})	1×10^{-5}
Specific yield (–)	0.1

the hydraulic parameter values of the aquifer. Each part of the time drawdown curve can be related to the timing and the part of the aquifer contributing water to the pumped borehole (Mansour et al., 2011). To illustrate this, the numerical model is used to produce the time drawdown curve and the release of water from an unconfined aquifer like the one illustrated in Figure 1a. Rushton, Connorton, and Tomlinson (1989) demonstrate that the fluctuation of the water table is within the upper 20 m of the aquifer. Beyond this depth, the hydraulic conductivity becomes small, and the aquifer becomes unproductive. Following Rushton, Connorton, and Tomlinson (1989), we focus here on the upper part of the aquifer, and we assume that the aquifer thickness is 20 m. The hydraulic parameter values of the aquifer are shown in Table 1. In the two examples below, no horizontal or vertical variations of hydraulic conductivity values are included in the model runs.

Figure 2a shows the time drawdown curve produced by pumping 2000 m^3/day for 10 days from a 0.1 m diameter borehole that is fully penetrating the aquifer. Figure 2b shows three curves representing the amount of water released from the well storage, the specific storage (the elastic storage of the aquifer) and the specific yield (water from the water table). Figure 2a,b is divided into four distinct time periods or zones reflecting different behaviours. Zone A corresponds to a nonlinear behaviour of the time drawdown curve shown in Figure 2a when most of the water is released from the pumped borehole storage and this decreases gradually allowing the water to be released mostly from the specific storage as illustrated in Figure 2b. Over the duration defined by zone B, the water is released from the elastic storage of the aquifer only and the time drawdown curve takes the shape of a straight line. Theis' solution (Theis 1935) can be applied over this part of the time drawdown curve. In Zone C, the water released from the specific storage starts to reduce and this is substituted by the release of water from the specific yield as shown in Figure 2b. In this case, the time drawdown curve takes a nonlinear shape as illustrated in Figure 2a. Finally, Zone D defines the time when all the water is released from the water table or the specific yield. The Theis solution can be applied here again but with using the specific yield value of the aquifer rather than the specific storage value.

Figure 2c,d shows the amount of water released from the elastic storage and the water table at different distances across the aquifer at 0.0005 day and 0.5 day, respectively. These two plots represent two snapshots of time during Zone B and Zone D, respectively. These figures illustrate how the released water takes the form of waves, which in case of Figure 2c, the wave represents water released from elastic storage only (Zone B), and of Figure 2d, the wave represents the water released from the water table (Zone D).

To illustrate the impact of the vertical hydraulic conductivity value (K_v) amongst other hydraulic parameter values on the behaviour of the time drawdown curve and on the source of water released from the aquifer, the model used above is rerun after reducing the value of K_v from 0.05 m/d to 0.005 m/d. Figure 3a shows the simulated time drawdown curve recorded at the pumped borehole. The lower $K_v$value causes an increased drop in water levels inside the pumped borehole with a maximum drawdown value of approximately 3.1 m at the end of the simulation period compared to approximately 2.6 m with the use of K_v value of 0.05 m/d as shown in Figure 2a.

Figure 3b shows a significant increase in the duration of Zone B, when the water is released from the elastic storage of the aquifer only and when Theis' solution can be applied. The increased duration of Zone B can be attributed to the higher vertical hydraulic head difference required between the nodes in the water table and those in the aquifer for the water table to start to respond. At time 0.0005 days, Figure 3c shows that the elastic storage is the only source of water similar to Figure 2c. However, the reduction of K_v value has also led to the increase of the duration of Zone C which represents the time during which the water is released from the water table and the elastic storage of the aquifer. This is also demonstrated by the plot shown in Figure 3d which shows that at time 0.5 day, unlike the plot in Figure 2d, the amount of water is released predominantly from the water table but also from the elastic storage of the aquifer.

2.3 | Equation Describing the Vertical Variation of K_v and Implemented in the Model

As the vertical hydraulic conductivity parameter plays a significant role in the calculation of the water level inside the pumped borehole, it is imperative that its variation with depth is also included in the LF models used to calculate the yield of boreholes under different climatic conditions. In weathered or fractured aquifers, the behaviour of the hydraulic system is expected to be different when the water table is close to the ground surface and the hydraulic system has high permeability, from its behaviour under drought conditions when the water table drops to low elevations and the groundwater system permeability is low. Although depth-dependent observations from the field show nonlinear variations in hydraulic conductivity values with depth, see, for example, Bianchi et al. (2020), for simplicity here we derive an equation controlling the vertical exchange of water between the water table assuming the aquifer hydraulic permeability reduces with depth linearly (Figure 4).

The vertical variation of the vertical hydraulic conductivity across the depth of the groundwater system is defined by the hydraulic

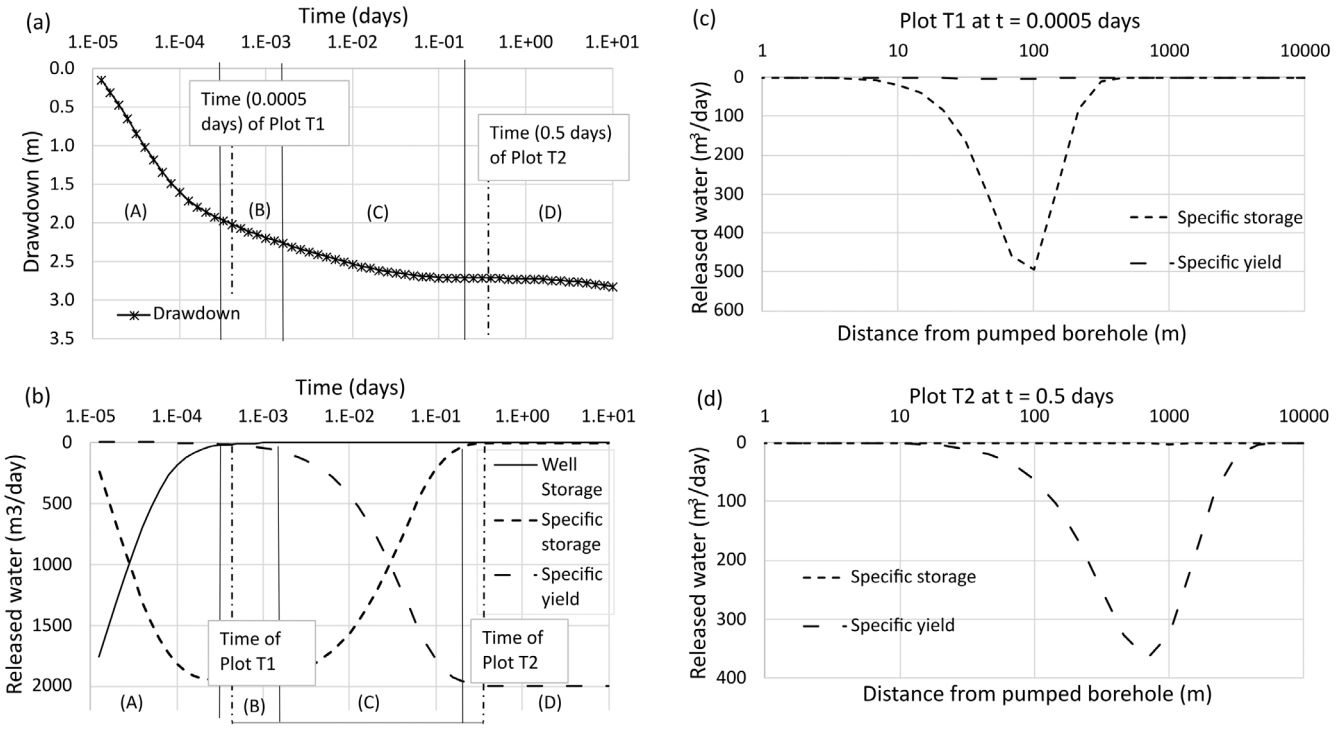

FIGURE 2 | (a) Time drawdown curve. (b) Plots of released water volumes with time. (c) Location and source of water released at 0.0005 days. (d) Location and source of water released at 0.5 days.

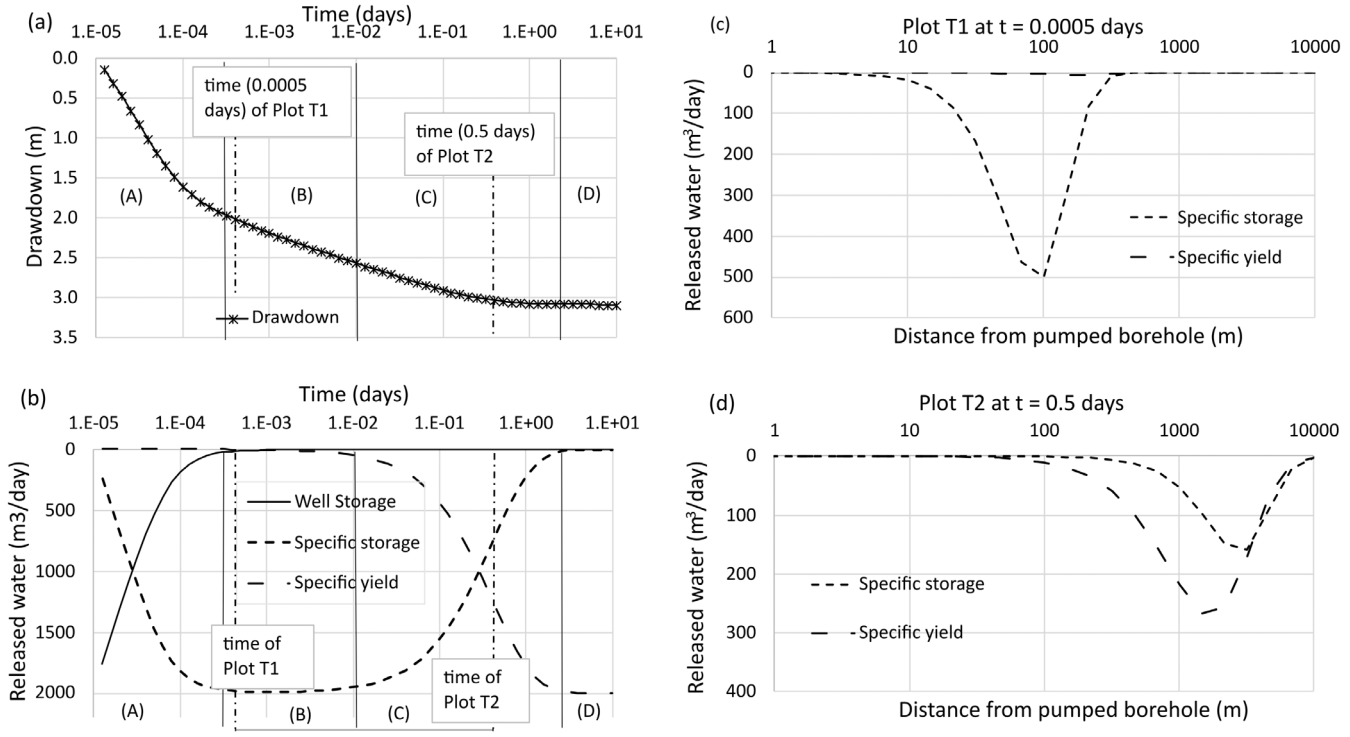

FIGURE 3 | (a) Time drawdown curve. (b) Plots of released water volumes with time. (c) Location and source of water released at 0.0005 days. (d) Location and source of water released at 0.5 days.

conductivity values at the top and base of the aquifers K_{v_ztop} and K_{v_zbase}, respectively. The linear increase of K_v from base to top is determined by the slope parameter m calculated as follows:

$$m = \left(K_{v\_ztop} - K_{v\_zbase}\right) / \left(z_{top} - z_{base}\right) \quad (3)$$

At any distance z (m) from the base of the aquifer, the vertical hydraulic conductivity is given by

$$K_{v\_z} = K_{v\_zbase} + \frac{\left(K_{v\_ztop} - K_{v\_zbase}\right)}{\left(z_{top} - z_{base}\right)}\left(z - z_{base}\right) \quad (4)$$

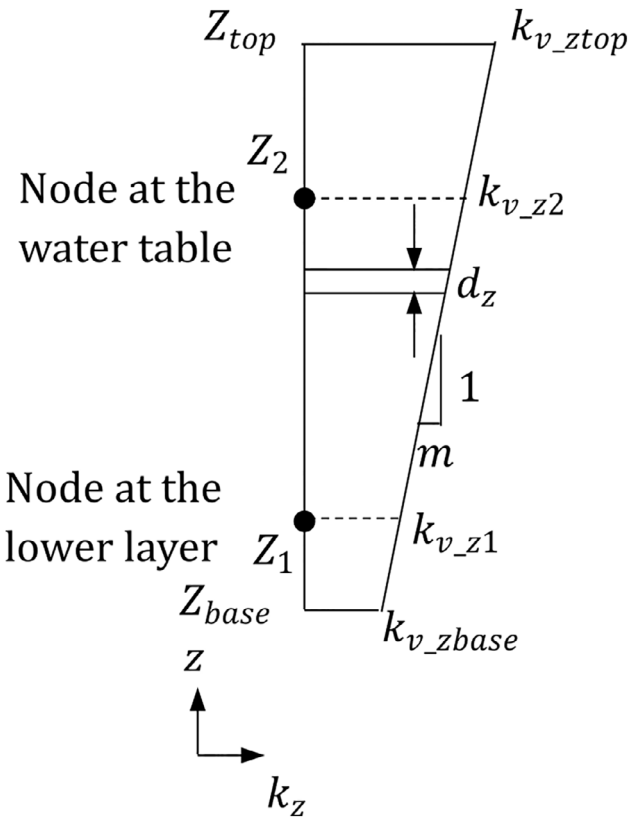

FIGURE 4 | A schematic showing the linear vertical variation of k_v with depth. k_v.

The vertical flow crossing the discrete volume with depth dz (Figure 4) is given by Darcy law as $q_v = K_{v\_z}\frac{dh}{dz}$. A relationship between the head and the vertical flow can be then derived by substituting for by K_{v_z} value from Equation 4:

$$dh = \frac{q_v}{K_{v\_z}}dz = \frac{q_v}{K_{v\_zbase} + m(z - z_{base})}dz \quad (5)$$

Integrating Equation 5 between Point 1 and Point 2 in Figure 4 yields the vertical flow between these two points. This is given by

$$q_v = \frac{m}{ln\left(\frac{K_{v\_zbase} + m(z_2 - z_{base})}{K_{v\_zbase} + m(z_1 - z_{base})}\right)}(H_2 - H_1) \quad (6)$$

From Equation 6, the general equation that gives the value of the conductance controlling the vertical flow between the two points 1 and 2 in Figure 4 is

$$C = \frac{m}{ln\left(\frac{K_{v\_zbase} + m(z_2 - z_{base})}{K_{v\_zbase} + m(z_1 - z_{base})}\right)} \quad (7)$$

Equation 7 is similar to the logarithmic mean transmissivity equation provided by Goode and Appel (1992) after Butler (1957) and Appel (1976). In addition, this equation is not singular when k_v is constant with depth, rather it converges to the value of $C = K_{v\_zbase} / (z_2 - z_{base})$ if $z_1 = z_{base}$.

3 | Results

3.1 | Significance of the Variation of the Vertical Hydraulic Conductivity on the Drawdown Time Series

The numerical radial flow model (Mansour et al., 2011, Ascott et al. 2019) has been updated to include the variation of K_v value based on the position of the water table. In the updated model, the vertical flows between the water table nodes and the aquifer nodes, as shown in Figure 1a, are calculated using the conductance values based on Equation 7. The significance of K_v value with depth is investigated using three examples detailed in Table 2. In the first two examples, the model is applied to simulate the time drawdown curves produced from a 10000 m circular aquifer with a depth of 20 m as illustrated in Figure 1a. The well diameter is assumed to be 0.1 m and is pumped for 10 days at a constant rate of 4650 m^3/day. The recovery of the drawdown values is recorded for a further 10 days. In these two examples, we study the impact of varying K_v with depth on time drawdown curves obtained from pumping tests. The difference between Examples 1 and 2 is the initial water table position which is assumed horizontal but at a depth of zero and seven meters, respectively.

The hydraulic parameter values are listed in Table 1. They consist of a horizontal hydraulic conductivity value of 50 m/d, a specific storage value of $S_s = 1 \times 10^{-5}\ m^{-1}$ and a specific yield of 0.1 [−]. However, the value of K_v is obtained from the profile illustrated in Figure 4 and is defined by the base K_v value $K_{v\_zbase} = 0.005\ m/d$ and the top K_v value $K_{v\_top} = 0.05\ m/d$. The slope of the profile defining the variation of K_v with depth is, therefore, 0.00225.

Figure 5a,b shows the time drawdown curves of the pumping and recovery phases simulated using Example 1, respectively, where the initial water table is set at depth zero from the aquifer top. Each plot contains two curves produced using a model with variations of K_v with depth and another where K_v (0.05 m/d) is constant with depth. These figures show that the curves are almost identical during the early times of the simulation but then they diverge at approximately 0.01 day with a maximum difference of approximately 0.7 m in the pumping phase at around 1.0 day (Figure 5a). This is approximately 10% of the drawdown observed when no vertical variation of K_v is included. The maximum difference between the curves in the recovery phase is approximately 0.6 m (Figure 5b) at around 0.001 days.

At time 0.1 day, the water table drops by 0.03 m below the top of the aquifer at the water table node adjacent to the pumped borehole (Node 1 in Figure 1a) when no vertical variation of K_v is included in the model. The elevation of Node 1 from the base of the aquifer is 19.97 m. The elevation of the node in the lower layer (Node 2 in Figure 1a) is 9.98 m as it moves down with Node 1 but at half the pace. When the variation of K_v with depth is included, the water table drops by 0.004 m from the top of the aquifer at Node 1 (Figure 1a) only. We will assume that the elevations of Node 1 and Node 2 from the base of the aquifer in this case are 20.0 m and 10.0 m, respectively, and by applying Equation 7,

TABLE 2 | Details of the three examples used to study the significance of the inclusion of the variation of the vertical hydraulic conductivity with depth.

Example	Details	Zone of water table fluctuation
1. Pumping test with the water table at the top of the aquifer at time zero	Q = 4650 m³/day for 10 days. Fluctuation of the water table within the wide part of the profile. Initial saturated thickness = 20 m Aquifer radius = 10 km $k_{v_{ztop}} = 0.05\ m/day$ $k_{v_{zbase}} = 0.005\ m/day$	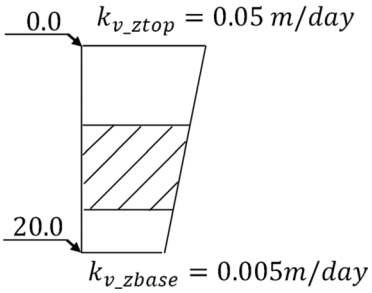
2, Pumping test with the water table at depth equal to 7 m at time zero	Q = 4650 m³/day for 10 days. Fluctuation of the water table within the narrow part of the profile. Initial saturated thickness = 13 m Aquifer radius = 10 km $k_{v_{ztop}} = 0.05\ m/day$ $k_{v_{zbase}} = 0.005\ m/day$	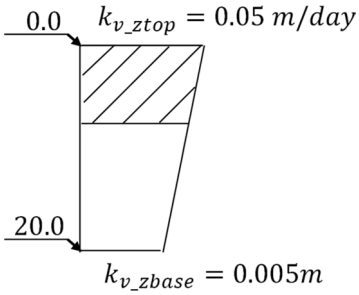
3. Long-term pumping with recharge for deployable output assessment. Water table at depth equal to 5 m at time zero	Q = 4650 m³/day with long pumping duration. Transient recharge rates with an average value of 0.52 mm/day. Fluctuation of the water table within the narrow part of the profile. Initial saturated thickness = 25 m Aquifer radius = 2 km $k_{v_{ztop}} = 5\ m/day$ $k_{v_{zbase}} = 0.5\ m/day$	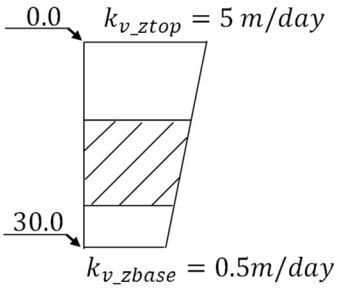 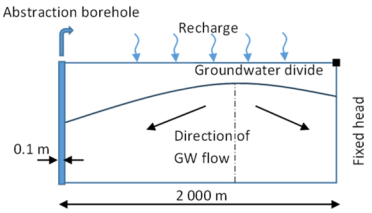

we find that the value of the conductance controlling the flow between these two nodes is equal to 0.0038 d^{-1}. Compared this with a conductance value of $C = 0.005\ d^{-1}$ calculated with constant K_v with depth indicates that for the same hydraulic gradient the vertical transfer of water between Node 1 and Node 2 is higher when there is no vertical variation in K_v. This is why the time drawdown curve produced with no vertical variation of K_v (the solid line in Figure 5a) becomes shallower than the time drawdown curve produced with vertical variation of K_v included (the dashed line), as more water is released from the water table rather than the elastic storage of the aquifer with no variation of K_v.

This is confirmed by the plots showing the water released from the specific yield spatially across the aquifer nodes in Figure 6a at time 0.1 days. At this time, the amount of water released from the water table is 1142 m³/day and 4134 m³/day with and without the inclusion of vertical variations of K_v in the model, respectively. To compensate for the lower amount of water received from the water table when the variations in K_v are included in the model, the water level drops more in the pumped well to establish higher hydraulic gradients in the lower layer, which leads for more water to be released from the elastic storage.

The increased drawdown values in the lower layer of the model with vertical variations in K_v leads to more vertical flow to be released from the water table at later times as shown in Figure 6b and Figure 6c. These figures show that the maximum water rates released from the water table with and without the vertical variation of K_v are close after 1.0 day. These are 4260 m³/day and 4640 m³/day, respectively (Figure 6b). These values become

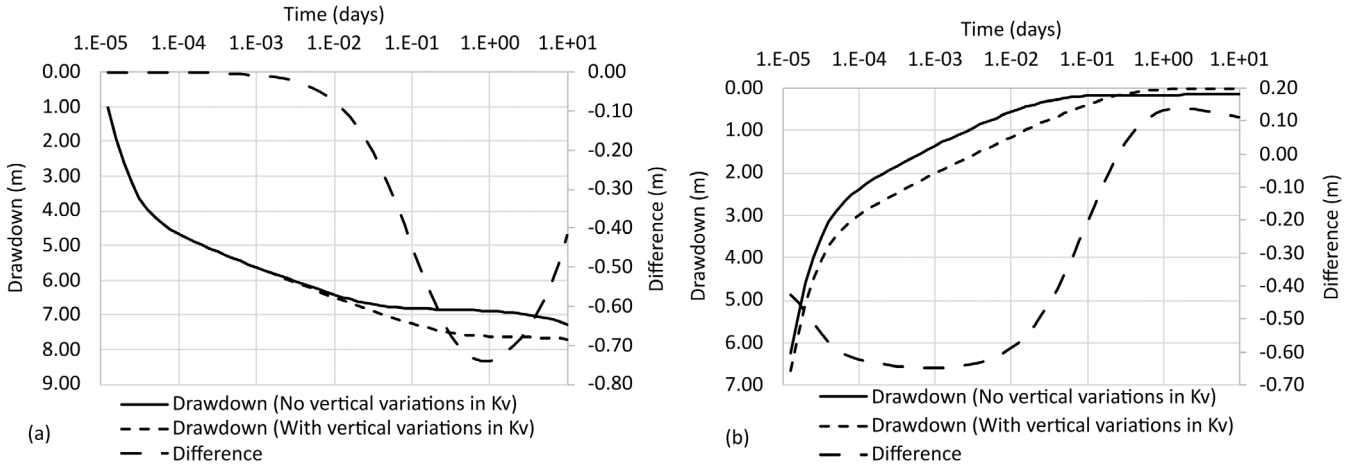

FIGURE 5 | Time drawdown curves with and without vertical variations of k_v. Initial conditions with the water table at the top of the saturated thickness (Example 1). (a) Pumping phase. (b) Recovery phase.

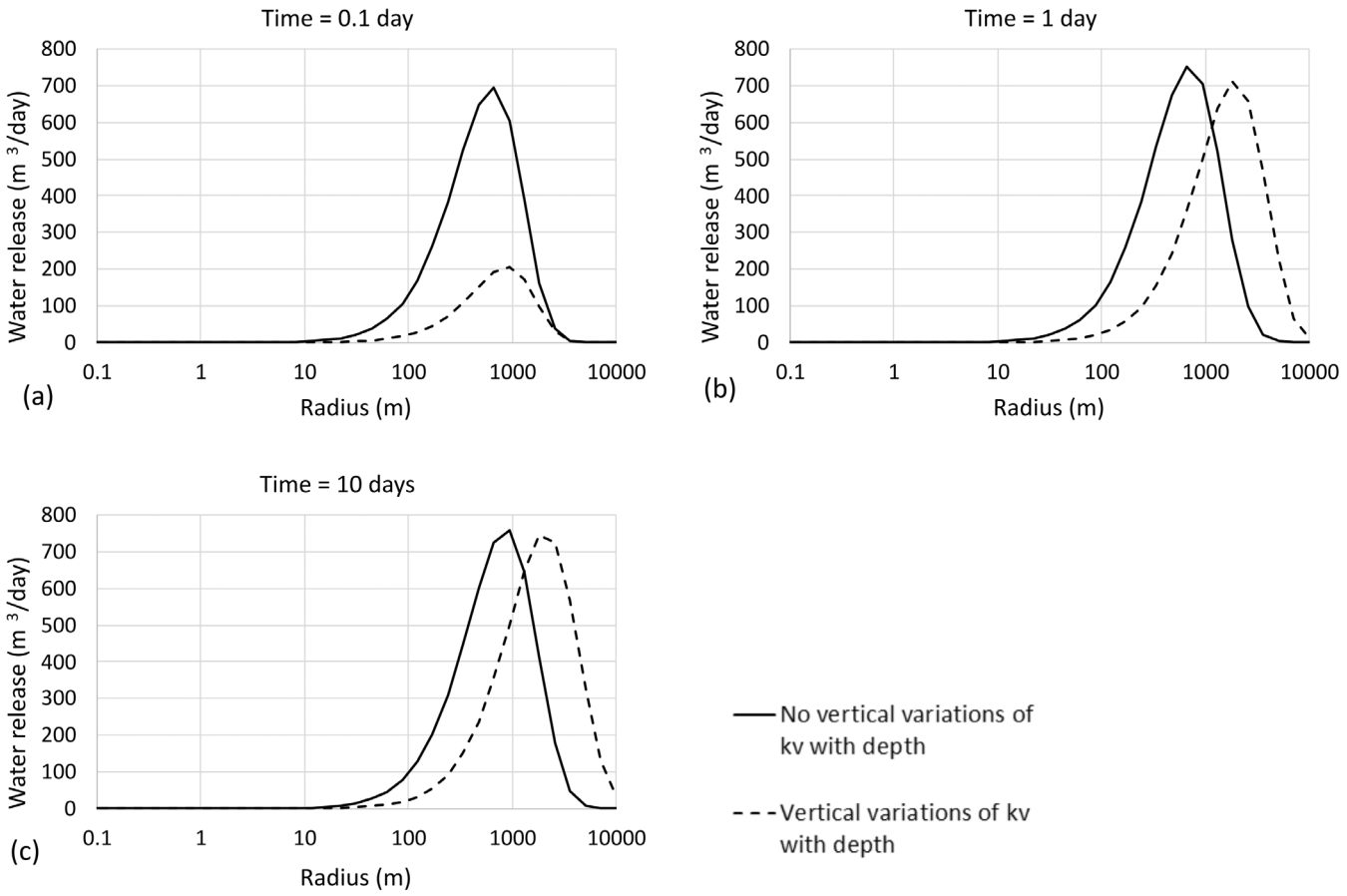

FIGURE 6 | Vertical water release from the water table nodes at 0.1, 1.0 and 10 days with and without the inclusion of the vertical variations in k_v. The initial water table location is at the top of the aquifer (Example 1).

equal to 4640 m^3/day in both cases at the end of the pumping phase (Figure 6c) but note that the location from where the water is released is different.

In Example 2, the initial water table elevation is set at 7 m from the top of the aquifer. The lowered water table position impacts the calculation of the conductance value from Equation 7 as the saturated thickness of the aquifer is significantly reduced. Figure 7a,b shows the time drawdown curves produced by the numerical models for the pumping and recovery phases, respectively. These figures show that the differences between the time drawdown curves are greater than those calculated in Example 1 with a maximum drawdown difference of approximately 1.2 m occurring at approximately 1.0 day after the onset of pumping (Figure 7a).

Figure 8 shows the plots of water released from the water table at 0.1, 1.0 and 10 days. Similar to what is observed in Example

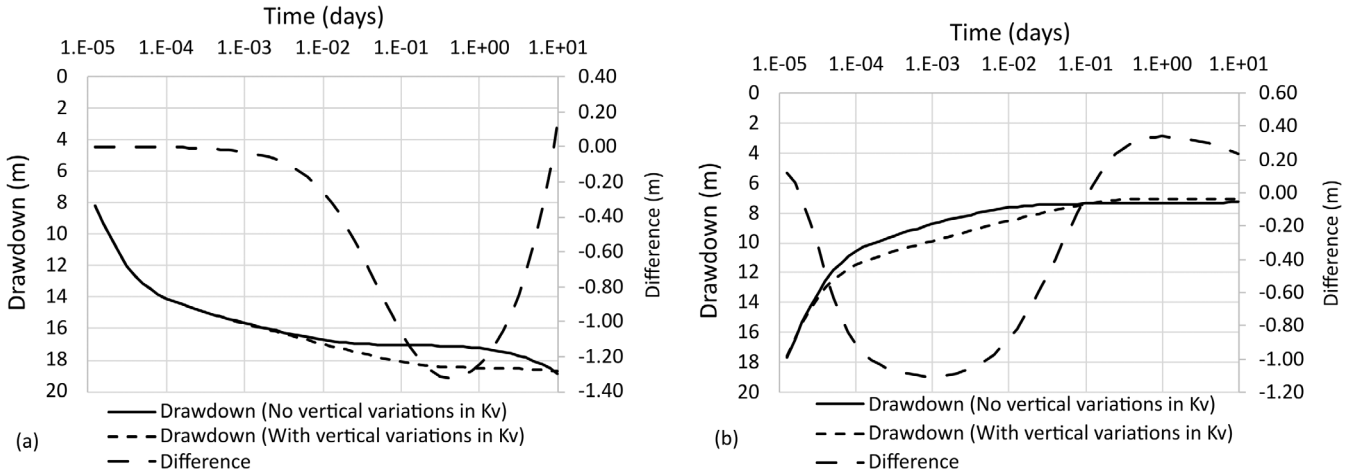

FIGURE 7 | Time drawdown curves with and without vertical variations of k_v. The initial conditions with the water table at 7 m below the top of the saturated thickness (Example 2). (a) Pumping phase. (b) Recovery phase.

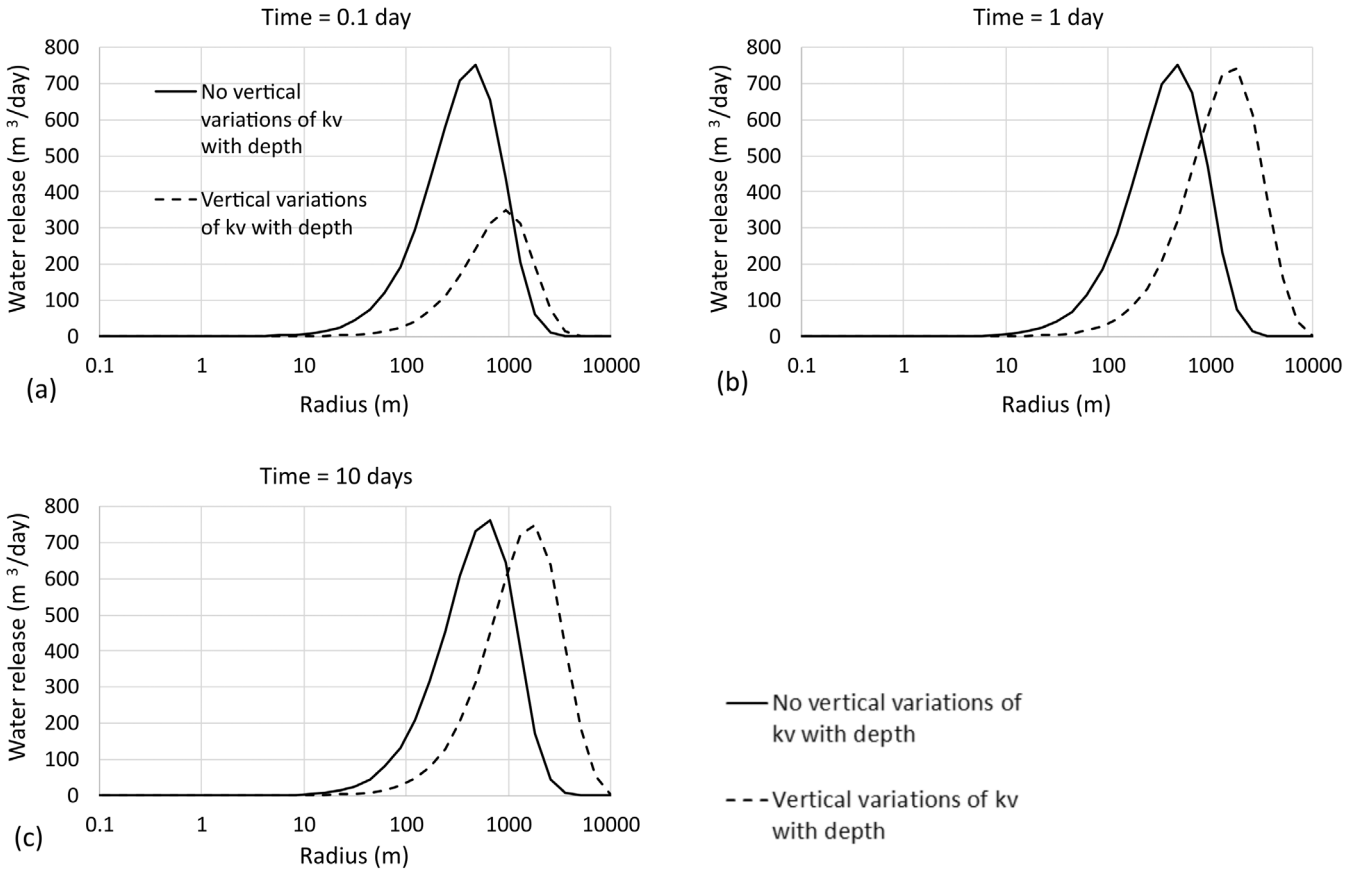

FIGURE 8 | Vertical water release from the water table nodes at 0.1, 1.0 and 10 days with and without the inclusion of the vertical variations in k_v. Initial water table location is at 7 m from the top of the aquifer (Example 2).

1, plots in Figure 8a show that at 0.1 day, the water released from the water table is higher when K_v is constant with depth (4626 m^3/day) than when K_v varies with depth (1954 m^3/day).

At the end of the pumping phase, 10 days, the simulated water table drops by 0.39 m and 2.45 m from its initial location of 7 m with and without the vertical variation of K_v, respectively. This has an important implication on the time drawdown curve recorded at the pumped borehole. The reduced saturated thickness in the case of no vertical variations in K_v causes the drawdown values at the borehole (the solid line in Figure 7a) to become higher than those calculated when K_v is varied with depth if longer pumping has taken place as will be demonstrated in Example 3. Figure 7a shows that the time drawdown curves from the two models converge to the same drawdown value at the pumping phase.

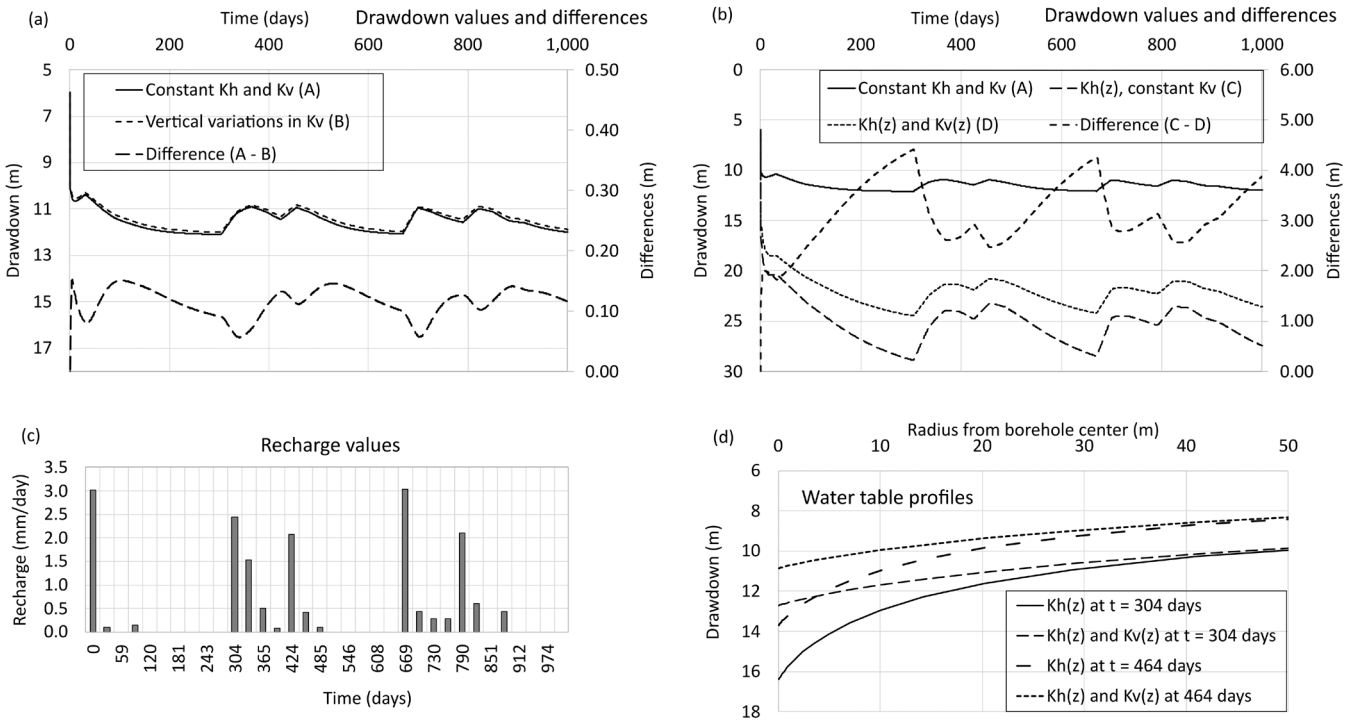

FIGURE 9 | (a) Time drawdown (TD) curves with and without variations of k_v and with no vertical variations in k_h. (b) TD curves with varying k_h with depth. (c) Time series of recharge values. (d) water table profiles at times 304 and 464 days. The initial conditions with the water table at 5 m below the top of the saturated thickness and with the inclusion of recharge (Example 3).

Example 3 represents the case when pumping takes place for a long time in an aquifer with varying K_v with depth and subject to recharge. We also use this example to demonstrate the significance of adding the vertical variations in K_v compared with the inclusion of vertical variations of K_h in the model.

In this example, we use an aquifer setting that is closest to that used by Ascott et al. (2019) and that addresses the calculation of drawdown values in a synthetic borehole representative to boreholes drilled in the Chalk aquifer in the UK. The hydraulic parameters are the same as in Example 1 and Example 2, but we set the vertical hydraulic conductivity to 5 m/day when K_v is constant with depth because usually K_v is assumed to be $1/10^{th}$ of the K_h value (50 m/day). The profile of vertical variations of K_v is defined by $K_{v\_base} = 0.5m/day$ and $K_{v_{top}} = 5\ m/day$ when K_v value is varied with depth (Table 2).

Monthly transient recharge values are uniformly applied at the top of the water table with an average recharge value of 0.52 mm/day. The aquifer extent had to be limited to 2 km to avoid excessive recharge going into the system and causing the water table to rise above the top of the aquifer. On average the total recharge is 6495 m^3/day, and the pumping rate is set to 4650 m^3/day. With the outer boundary defined by a fixed head to set the initial position of the water table at 5 m, the location of groundwater divide is checked during the simulation to make sure it does not reach the fixed head outer boundary, consequently, the water pumped at the borehole is released from the aquifer storage at all times. The aquifer thickness in this example is increased to 30 m which gives a saturated thickness of 25 m with the water table located at 5 m below the top of the aquifer at the onset of pumping.

Figure 9a shows the time drawdown curves simulated using models with and without the vertical variation of K_v and for a simulation period of 1000 days. These curves fluctuate similarly to each other due to recharge (Figure 9c). The difference between the two curves is not constant with time as shown by the third curve in Figure 9a with a maximum difference of approximately 0.13 m.

When the vertical variation in K_h is added, the time drawdown values (the lowest dashed line in Figure 9b) become significantly higher than the case when no vertical variations in K_h or K_v (the solid line in Figure 9b). This indicates that the inclusion of the variation of K_h is much more important than the variation of K_v with depth. However, Figure 9b shows that the addition of the vertical variations of both K_h and K_v produce a time drawdown curve that is at higher elevation than the drawdown curve produced by varying K_h only. The maximum difference between these two curves is approximately 4.2 m and shows that the vertical variations in K_v affect the drawdown values when varying K_h with depth.

Figure 9a,b shows that the time drawdown curves at the pumped borehole fluctuate at a higher elevation (lower drawdown values) when the vertical variations in K_v are included in the model. This is caused by the increased saturated thickness as the water table is located at higher elevations as shown by the water table profiles plotted at two different time steps in Figure 9d. In this case, lower horizontal hydraulic gradients in the lower layer of the numerical model are required to satisfy the pumping rate specified at the pumped borehole.

4 | Discussion

In this study, we update the numerical radial flow model to add the variation of the vertical hydraulic conductivity value with depth and we investigate the significance of this addition to the model output. It has been shown that the implementation of the variation of K_v with depth does not make significant impact on the simulated time drawdown curve at the early times of the pumping test. However, it has an important impact on the simulated time drawdown curve at the later times of test. In addition, larger differences are recorded when the water table is lowered to a depth close to the middle of the aquifer. However, in both cases, the differences between the time drawdown curves produced with and without the variations of K_v was insignificant two hours since the onset of pumping. Although this is highly dependent on the hydraulic parameter values of the aquifer, for short pumping test, the inclusion of vertical variations of K_v with depth may not be important.

The impact of the implementation of the vertical variation of K_v only, in a model that simulates the water level fluctuations inside a pumped borehole to study deployable output, is also found to be insignificant. The maximum differences between the two time-drawdown curves simulated with and without K_v variation with depth is approximately 0.14 m. This is a small value compared with the increase of drawdown values caused by adding vertical variations in K_h with depth, which causes the time drawdown curve to drop by more than 15.0 m. However, it has been demonstrated that varying K_v with depth is important when K_h is varied with depth. Another important hydraulic process, which is the vertical variations of the storage coefficient value with depth is expected to affect the water levels inside the pumped borehole (Rushton and Chan 1976) and is planned to be included in the model in future developments.

The addition of variations of K_v with depth produced higher drawdown values after two hours of pumping in Example 1 and Example 2. In contrast, we see that this reduces the drawdown values in Example 3. This indicates that the groundwater flow processes resulting from the addition of K_v variation with depth are complex and depend on the vertical conductance values connecting the water table and the lower layer in the model, the location of the water table, the other aquifer hydraulic parameter values, and the timing from pumping onset. In Example 3, transient recharge is added and the model is run for a longer period of time. The recharge and pumping cause a change in the curvature of the water table with the peak value representing the location of the groundwater divide. Part of the infiltrated water is pumped by the borehole and the remaining discharge at the outer boundary. To avoid outer boundary influence on the time drawdown curve due to the selected dimension of the aquifer, the location of the groundwater divide is checked during the simulation to ensure that no water is withdrawn from that outer boundary at any time.

The vertical variation of K_v implemented in this model is assumed linear with a high value at the top of the saturated depth and low value at the base of the saturated depth as illustrated in Figure 4. More complex profiles of the vertical variations of K_v with depth can be considered. One approach is to use a polynomial equation to represent this variation. Bianchi et al. (2020) show profiles of physical heterogeneity in weathered basement aquifers in Ghana. The variation of the hydraulic conductivity with depth represented by these profiles can be approximated by third-degree polynomials. These polynomials can be used to derive equations equivalent to Equation 7 to calculate the conductance value that controls the volume of water moving between the nodes in the vertical direction in a LF numerical model discussed here.

5 | Conclusions

The simplification of numerical models and the use of LF models is a common practice to overcome numerical instabilities and to reduce the run time of numerical models. The improved model performance is of significant importance when the model is applied to simulate the impact of large number of climate scenarios to study and manage future groundwater resources by calculating the groundwater levels inside pumped boreholes. Here we add the variations of the vertical hydraulic conductivity value with depth to a numerical radial groundwater model used in the simplest configuration possible. Usually, K_v variations with depth have been overlooked in simplified numerical models prepared at either borehole or regional scales. We demonstrate that the addition of this mechanism in the numerical model code has a minor impact on the time drawdown curves produced from relatively short pumping tests. However, its impact appears to be important when the drawdown values are affected by infiltration recharge and the simulation is run for a long time to assess deployable output. In addition, the variation of K_v with depth when K_h is also varied with depth had a major impact on the water levels simulated inside the pumped borehole.

In this study, the vertical hydraulic conductivity value is assumed to vary linearly with depth. This simplification allows a straightforward derivation of the equation used to calculate the vertical conductance value (Equation 7). A more complex profile can be used if a continuous mathematical equation can be found to represent the shape of the profile. This extends the application of the method to an international context enabling hydrogeological complexity to be represented using a polynomial approximation.

Ideally, we would compare the method against the observed, however, suitable data are not readily available, which limited our ability to achieve this. We present an example of a methodology that can be used with most codes; cartesian models as well as the radial flow model presented in the article and where vertical variation of hydraulic properties occurs in aquifers. We plan to extend the method to address vertical storage changes with depth and to use the methodology on appropriate observed data as applicable.

Acknowledgements

The authors would like to thank the anonymous reviewers and the editor for their valuable comments to improve the manuscript. This work

has been inspired by the work of M Mansour and A Hughes' PhD supervisor, Dr. A.E.F. Spink, whose contribution is acknowledged posthumously. M Mansour would like to thank Ms. Carol Assi for reading the initial draft of the paper. This work was supported by the Hydro-JULES research programme (NERC National Capability funding Grant number: NE/X019063/1) and the National Capability NEE4991S Process Modeling Team project (UKRI). This work is published with the permission of the Executive Director, British Geological Survey (UKRI).

Data Availability Statement

The radial flow model used to simulate groundwater levels is developed at The University of Birmingham and the British Geological Survey. The authors can make the executable and the data produced for this paper available for research purposes.

References

Appel, C. A. 1976. "A Note on Computing Finite Difference Interblock Transmissivities." *Water Resources Research* 12, no. 3: 561–563. https://doi.org/10.1029/WR012i003p00561.

Ascott, M. J., M. M. Mansour, J. P. Bloomfield, and K. A. Upton. 2019. "Analysis of the Impact of Hydraulic Properties and Climate Change on Estimations of Borehole Yields." *Journal of Hydrology* 577: 123998. https://doi.org/10.1016/j.jhydrol.2019.123998.

Asher, M. J., B. F. W. Croke, A. J. Jakeman, and L. J. M. Peeters. 2015. "A Review of Surrogate Models and Their Application to Groundwater Modeling." *Water Resources Research* 51, no. 8: 5957–5973. https://doi.org/10.1002/2015WR016967.

Beeson, S., B. D. Misstear, and J. J. van Wonderen. 1997. "Assessing the Reliable Outputs of Groundwater Sources." *Water and Environment Journal* 11, no. 4: 295–304. https://doi.org/10.1111/j.1747-6593.1997.tb00132.x.

Bianchi, M., A. M. MacDonald, D. M. J. Macdonald, and E. B. Asare. 2020. "Investigating the Productivity and Sustainability of Weathered Basement Aquifers in Tropical Africa Using Numerical Simulation and Global Sensitivity Analysis." *Water Resources Research* 56, no. 9: e2020WR027746. https://doi.org/10.1029/2020WR027746.

Boulton, N. S. 1954. "The Drawdown of a Water-Table Under Non-steady Conditions Near a Pumped Well in an Unconfined Formation." In *Proceedings of the Institution of Civil Engineers 3, Part 3*, 564–579.

Butler, S. S. 1957. *Engineering Hydrology: Prentice-Hall*, 356. NJ: Englewood Cliffs.

Calow, R., A. MacDonald, A. L. Nicol, and N. Robins. 2010. "Ground Water Security and Drought in Africa: Linking Availability, Access and Demand." *Groundwater* 48, no. 2: 246–256. https://doi.org/10.1111/j.1745-6584.2009.00558.x.

Christelis, V., and A. G. Hughes. 2022. "Multifidelity Surrogate Models for Efficient Uncertainty Propagation Analysis in Salars Systems." *Frontiers in Water* 4: 827036. https://doi.org/10.3389/frwa.2022.827036.

Christelis, V., G. Kopsiaftis, R. G. Regis, and A. Mantoglou. 2023. "An Adaptive Multi-Fidelity Optimization Framework Based on Co-Kriging Surrogate Models and Stochastic Sampling With Application to Coastal Aquifer Management." *Advances in Water Resources* 180: 104537. https://doi.org/10.1016/j.advwatres.2023.104537.

Goode, D. J., and C. A. Appel. 1992. Finite-difference interblock transmissivity for unconfined aquifers and for aquifers having smoothly varying transmissivity. U.S. Geological Survey Water -Resources Investigations Report 92–4124 https://doi.org/10.3133/wri924124.

Grout, M. W., D. W. Alexander, and R. J. Simpson. 1992. "Practical Aspects of Yield Investigations of Groundwater Sources." *Water and Environment Journal* 6: 397–407. https://doi.org/10.1111/j.1747-6593.1992.tb00769.x.

Harbaugh, A. W. 2005. MODFLOW-2005, The U.S. Geological Survey modular ground-water model—the Ground-Water Flow Process: U.S. Geological Survey Techniques and Methods 6–A16, variously p https://doi.org/10.3133/tm6A16.

Jackson, C. R. 2002. "The Variation of Hydraulic Conductivity With Depth in the Object-Oriented Groundwater Model ZOOMQ3D." *British Geological Survey*: 74pp. (CR/02/152N) (Unpublished). https://nora.nerc.ac.uk/9299/1/CR_02_152N.pdf.

Langevin, C. D., J. D. Hughes, A. M. Provost, et al. 2022. MODFLOW 6 Modular Hydrologic Model version 6.3.0: U.S. Geological Survey Software Release, 4 March 2022 https://doi.org/10.5066/P97FFF9M.

Mansour, M. M., A. G. Hughes, and A. E. F. Spink. 2007. *User Manual for the Layered R-Theta Numerical Model (COOMPuTe)*, 71. Nottingham, UK: British Geological Survey. (OR/07/029) (Unpublished). https://nora.nerc.ac.uk/id/eprint/13011/.

Mansour, M. M., A. G. Hughes, A. E. F. Spink, and J. Riches. 2011. "Pumping Test Analysis Using a Layered Cylindrical Grid Numerical Model in a Complex, Heterogeneous Chalk Aquifer." *Journal of Hydrology* 401: 14–21. https://doi.org/10.1016/j.jhydrol.2011.02.005.

Misstear, B. D. R., and S. Beeson. 2000. "Using Operational Data to Estimate the Reliable Yields of Water-Supply Wells." *Hydrogeology Journal* 8, no. 2: 177–187. https://doi.org/10.1007/s100400050004.

Neuman, S. P. 1972. "Theory of Flow in Unconfined Aquifers Considering Delayed Response of the Water Table." *Water Resources Research* 8, no. 4: 1031–1045.

Owor, M., J. Okullo, H. Fallas, A. M. Macdonald, R. Taylor, and D. J. MacAllister. 2022. "Permeability of the Weathered Bedrock Aquifers in Uganda: Evidence From a Large Pumping-Test Dataset and Its Implications for Rural Water Supply." *Hydrogeology Journal* 30: 2223–2235. https://doi.org/10.1007/s10040-022-02534-0.

Rushton, K. R., and Y. K. Chan. 1976. "Pumping Test Analysis When Parameters Vary With Depth." *Ground Water* 14, no. 2: 82–87. https://doi.org/10.1111/j.1745-6584.1976.tb03637.x.

Rushton, K. R., B. J. Connorton, and L. M. Tomlinson. 1989. "Estimation of the Groundwater Resources of the Berkshire Downs Supported by Mathematical Modeling." *Quarterly Journal of Engineering Geology* 22: 329–341.

Rushton, K. R., and K. S. Rathod. 1981. "Aquifer Response due to Zones of Higher Permeability and Storage Coefficient." *Journal of Hydrology* 50: 299–316.

Soley, R. W. N., T. Power, R. N. Mortimore, et al. 2012. "Modeling the Hydrogeology and Managed Aquifer System of the Chalk Across Southern England." *Geological Society of London, Special Publication* 364, no. 1: 129–154. https://doi.org/10.1144/sp364.10.

Tamayo-Mas, E., M. Bianchi, and M. M. Mansour. 2018. "Impact of Model Complexity and Multiscale Data Integration on the Estimation of Hydrogeological Parameters in a Dual Porosity Aquifer." *Hydrogeology Journal* 26, no. 6: 1917–1933. https://doi.org/10.1007/s10040-018-1745-y.

Theis, C. V. 1935. "The Relation Between the Lowering of the Piezometric Surface and the Rate and Duration of Discharge of a Well Using Groundwater Storage." In *Transactions of the American Geophysical Union, 16th Annual Meeting*, 519–524.

Upton, K. A., C. R. Jackson, A. P. Butler, and M. A. Jones. 2020. "An Integrated Modeling Approach for Assessing the Effect of Multiscale Complexity on Groundwater Source Yields." *Journal of Hydrology* 588: 125113. https://doi.org/10.1016/j.jhydrol.2020.125113.